The Potential Role of Systemic Buffers in Reducing Intratumoral Extracellular pH and Acid-Mediated Invasion

Ariosto S. Silva,[1] Jose A. Yunes,[1] Robert J. Gillies,[2] and Robert A. Gatenby[2]

[1]Laboratório de Biologia Molecular, Centro Infantil Boldrini, Campinas, Sao Paulo, Brazil and [2]Departments of Radiology and Integrative Mathematical Oncology, Moffitt Cancer Center, Tampa, Florida

Abstract

A number of studies have shown that the extracellular pH (pHe) in cancers is typically lower than that in normal tissue and that an acidic pHe promotes invasive tumor growth in primary and metastatic cancers. Here, we investigate the hypothesis that increased systemic concentrations of pH buffers reduce intratumoral and peritumoral acidosis and, as a result, inhibit malignant growth. Computer simulations are used to quantify the ability of systemic pH buffers to increase the acidic pHe of tumors in vivo and investigate the chemical specifications of an optimal buffer for such purpose. We show that increased serum concentrations of the sodium bicarbonate (NaHCO₃) can be achieved by ingesting amounts that have been used in published clinical trials. Furthermore, we find that consequent reduction of tumor acid concentrations significantly reduces tumor growth and invasion without altering the pH of blood or normal tissues. The simulations also show that the critical parameter governing buffer effectiveness is its pK_a. This indicates that NaHCO₃, with a pK_a of 6.1, is not an ideal intratumoral buffer and that greater intratumoral pHe changes could be obtained using a buffer with a pK_a of ~7. The simulations support the hypothesis that systemic pH buffers can be used to increase the tumor pHe and inhibit tumor invasion. [Cancer Res 2009;69(6):2677–84]

Introduction

A number of studies using pH-sensitive magnetic resonance imaging contrast agents, microelectrodes, and magnetic resonance spectroscopy with hyperpolarized C-13 have consistently shown that the extracellular pH (pHe) of tumors is significantly lower (6.6–7.0) than that of healthy tissues (7.2–7.4; refs. 1–4). This acidity is primarily due to (a) anaerobic glycolysis in tumor regions subjected to short-term or long-term hypoxia as a result of poorly organized vasculature with diminished chaotic blood flow, and (b) aerobic glycolysis (the Warburg effect), a common cancer phenotypic property in which the glycolytic metabolic pathways are used even in the presence of oxygen (5).

An acidic pHe induces pleiotropic changes in tumor cells. In many tumor types, acute or chronic incubation in a low-pH microenvironment increases invasiveness both in vitro and in vivo (6). Hill and Rofstad (7–9) have shown that lowering culture pH to 6.7 resulted in a 4-fold increase in the number of in vivo metastases of the treated cells compared with controls after tail vein injection.

In addition, a variety of cancer cell populations, when exposed to an acidic environment, have been shown to increase expression of interleukin-8 (IL-8), vascular endothelial growth factor (VEGF), carboninc anhydrase IX, lactate dehydrogenase, cathepsin B, matrix metalloproteinase (MMP)-2, and MMP-9 (10–13), all of which are associated with increased tumor growth and invasion in vivo. Interestingly, tumor cells are typically able to maintain high proliferation rates even in an acidic environment (14). An acidic pHe, on the other hand, induces significant toxicity in normal cells by reducing proliferation (14) and promoting apoptosis via a p53-dependent pathway (15) initiated by increasing caspase activity (16). In addition, an acidic pHe in normal tissues increases degradation of the extracellular matrix due to the production and release of proteolytic enzymes (10), promotes angiogenesis through the release of VEGF (12), and limits immune response to tumor antigens (17).

These findings have been synthesized into the acid-mediated tumor invasion model, which proposes that intratumoral acidosis results in flow of H⁺ ions along concentration gradients into normal tissue adjacent to the tumor. This produces a peritumoral ring of dead and dying cells and degraded extracellular matrix into which the still viable malignant cells invade (18, 19). The model is supported by experimental evidence showing a peritumoral acid gradient associated with normal cell apoptosis and extracellular matrix degradation (18, 19). Indirect support for this model is seen in a number of clinical studies, including (a) observations of increased glucose uptake on [¹⁸F]fluorodeoxyglucose positron emission tomography scans (and, therefore, increased acid production) in the transition from in situ to invasive cancer (20, 21) and that a higher level of uptake in many cancer types confer poor prognosis (22–24); (b) increased intratumoral lactate concentration is associated with poor prognosis (25, 26); and (c) increased expression of proteins that are up-regulated by acidic pHe (including IL-8, cathepsin B, lactate dehydrogenase, and carbonic anhydrase IX; refs. 10–14) is associated with poor prognosis (27–31).

If intratumoral acidosis facilitates invasion, a reasonable extension of the acid-mediated invasion model leads to the hypothesis that reduction of intratumoral and peritumoral acid concentrations may inhibit malignant tumor growth. Sodium bicarbonate (NaHCO₃) is one of the many physiologic buffers used to control the pH in blood and tissues. Excess H⁺ combines with bicarbonate and generates water and CO_2. Conversely, in environments wherein CO_2 is produced in excess, there is production of bicarbonate and free protons (Fig. 1) from carbon dioxide hydration. Previous studies (32, 33) showed that the levels of CO_2 are higher and concentrations of bicarbonate are lower in tumors than in blood or in healthy tissues.

In this article, we examine the effects of increased serum NaHCO₃ concentrations on intratumoral pHe and the consequent changes in the simulations of tumor growth. We then explore the
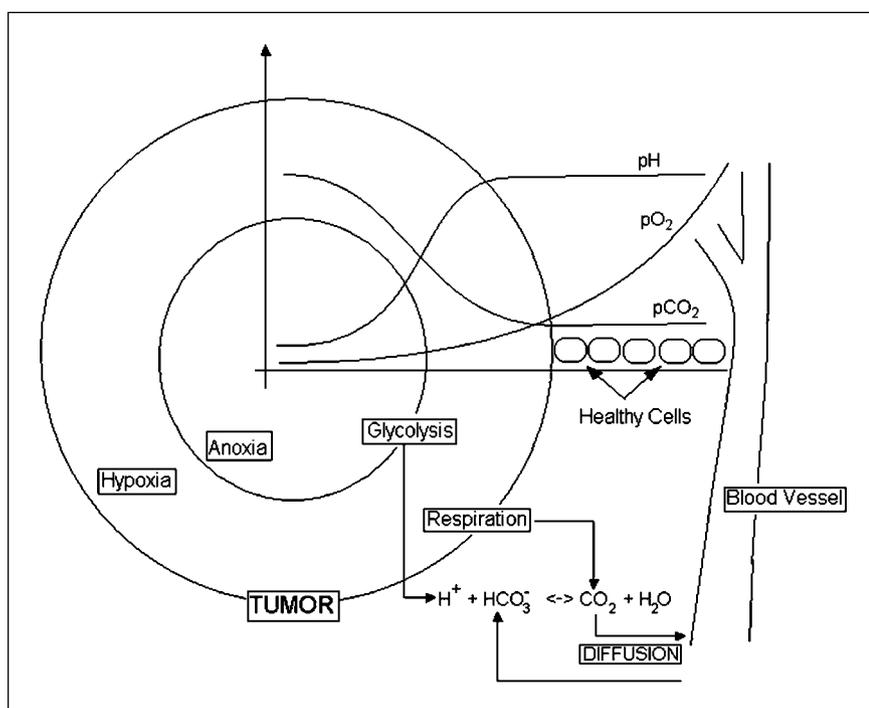
Figure 1. Tumor microenvironment. An avascular tumor with regions of hypoxia and anoxia produces both carbon dioxide from respiration and protons from anaerobic glycolysis. Bicarbonate buffers the pHe in the tissue by converting protons into water and carbon dioxide; the latter diffuses back to blood vessels and is expelled in the lungs.

chemical specifications of hypothetical buffers to determine the characteristics of an optimal buffer that may be more efficient than bicarbonate in inhibiting cancer invasion. The critical parameters tested are the dissociation constant (pK_a) and the diffusion coefficient.

Many computer and mathematical models have been created to represent the growth and interaction of tumors and healthy tissue (34–36), but none have considered the effects of buffers such as bicarbonate and phosphates.

In this work, we used a three-dimensional computer model, which represents a tumor as a spheroid with a diameter of 60 cells, embedded in a healthy vascularized tissue represented as a cubic volume 80 cells wide (Fig. 2). This model was analyzed using a tool developed for tissue simulation (TSim),[3] which calculates metabolic reactions, diffusion of species, and buffering effect, as well as cell duplication and apoptosis. The major advantages of using such a representation of the tumor-host environment are as follows: (*a*) The actual dynamics of the tumor-host interactions are better illustrated by a tridimensional model than by a flattened two-dimensional representation of it, and (*b*) this representation allows interrogation of the forces that shape the progression or regression of tumors (acidity, energetic metabolism, etc.) without the need of deep mathematical knowledge. This modeling technique is thus able to examine the complex, multiscalar, dynamic, and mutual interactions of molecular, cellular, tissue, and systemic parameters that affect cancer growth and therapy.

Materials and Methods

Model. Our focus in the modeling work is on small tumors (diameter of ∼1.5 mm) to investigate the potential for increased bicarbonate concentrations to delay the development of metastases or the transition from microinvasive to clinically apparent primary cancers. Due to the computational effort needed to simulate this model, we chose to represent

---

[3] http://www.i-genics.com

a fraction of the tumor (one eighth), considering that the tumor mass is symmetrical (Fig. 2).

It is well known that most tumors are spatially heterogeneous so that this represents a limitation in this model. However, clinical observations have shown that, in the tumor size used in these simulations, the assumption of homogeneity in tumor cell population is reasonable (37). The dimension of the tumor in this study is also comparable with small tumors implanted in window chambers in mice (19) and, thus, is valid for comparisons of pHe gradients observed in these experiments.

In our model, the cancer cells are more resistant to low pHe than normal cells. In previous works (34), the pHe threshold for death of tumor cells was described as being as low as 6.0, but in this work, we used a more conservative estimation of 6.4 while normal cells will not survive in an pHe lower than 6.8.

Tumor cells present increased glucose uptake and metabolism even in the presence of oxygen (38). In this study, we considered three cases wherein aerobic glucose metabolism of tumor cells was increased 10-, 50-, and 100-fold compared with normal cells (34) corresponding to the values in Supplementary Table S6.

Each cell is considered to be of cubic volume with side length of 25 μm to simplify the calculation of the diffusion of species (35). The species considered in this study are glucose, O_2, CO_2, H^+, bicarbonate anion, and a hypothetical buffer to test the tumoral pHe effect of adding a non–CO_2-generating buffer with different pK_a and diffusion rate. In this model, the concentrations of these species are considered to be constant in the blood vessels.

Diffusion. The simulation process is composed of two steps: (*a*) diffusion of the species and (*b*) cellular activities, including metabolism, proliferation, and death (Fig. 3). The former occurs at a much faster time scale than the latter, allowing them to be temporally separated in the simulations.

The diffusion was calculated with an approximation algorithm, which applies the definition of diffusion coefficient to each volume in the simulated space at 0.1-s intervals. The process was repeated 10 times to obtain the equilibrium concentrations of species over 1 s.

$$C_{t+1} = C_t - \left(C_t \times 6 - \sum_{i=1}^{6} C_{it} \right) \times D_N, \tag{A}$$

Figure 2. TSim graphical user interface view of the tumor model. *Blue,* one eighth of the tumor sphere. *Pink,* healthy tissue perfused by blood vessels (*red*). Simulations allow tumor growth to be simulated along with regional variations in pHe, as well as O_2, CO_2, and glucose concentrations and intracellular ATP.
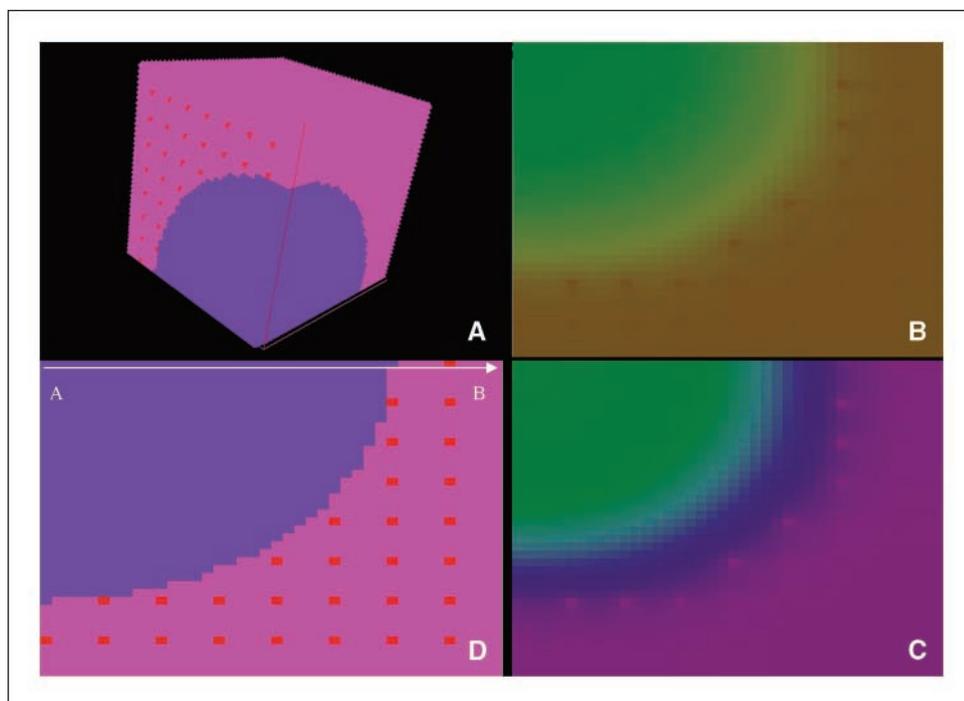
where C_t and C_{t+1} are the concentrations of the species in a volume at times t and $t + 1$, respectively; C_{it} is the concentration of the species in a neighboring volume in time t; and D_N is the diffusion coefficient normalized to the surface between two volumes ($25 \times 25 \, \mu m$) at one tenth of a second as time frame.

Metabolism, cell duplication, and cell death. Once the diffusion steps have been calculated, the software simulates the uptake of glucose and oxygen, glucose metabolism in either aerobic or anaerobic paths and the production of CO_2 or lactic acid corresponding to an interval of 1 s of simulated time.
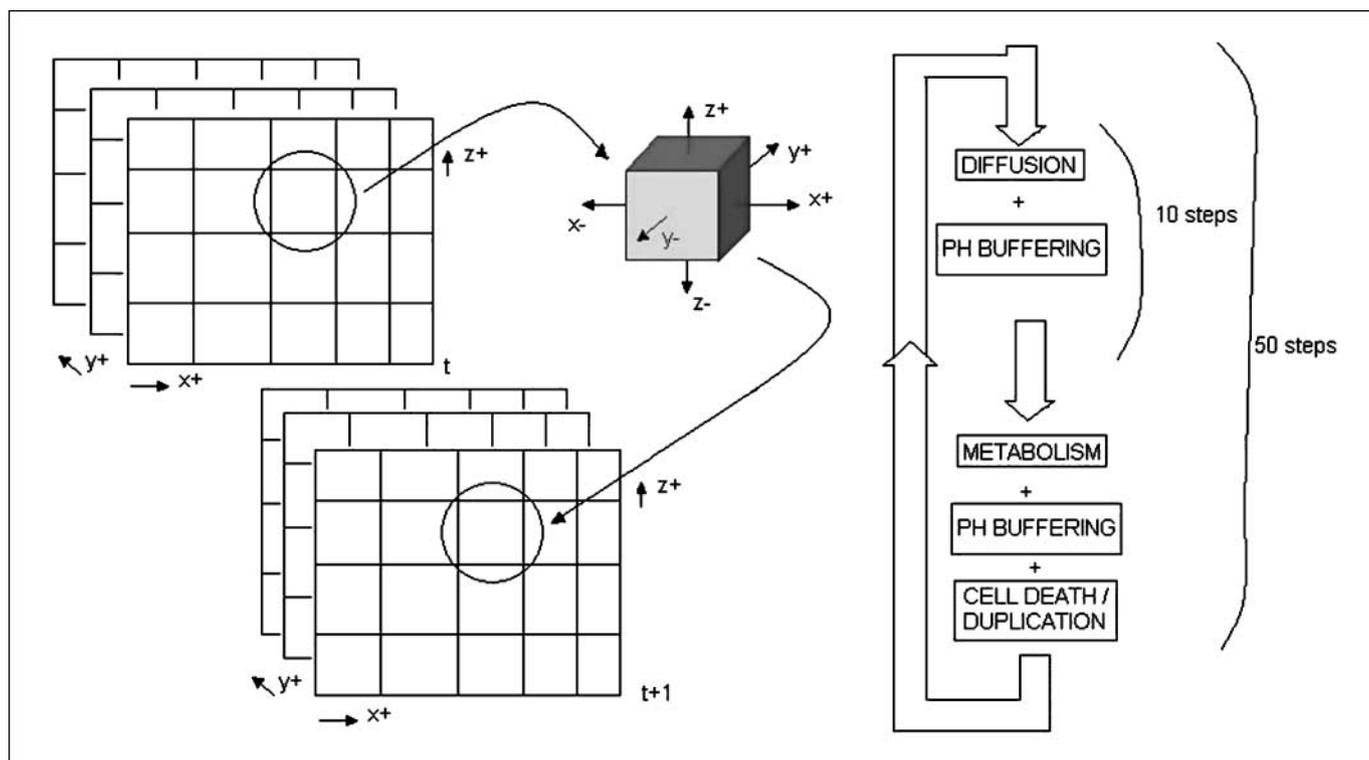
Figure 3. For each volume in simulation space at time t, the diffusion, metabolism, cell duplication, and death are calculated and the updated model is stored in the respective volume at time $t + 1$. Diffusion is calculated through an approximate algorithm with steps of one tenth of a second. Each generation of the simulation is composed of 50 metabolic steps, after which the decision is made on cell fate: duplication, death, or remain as is.

The uptake of glucose and O_2 is proportional to the concentration of these species in the extracellular environment. The transport of O_2 into the cell is due to simple Fickian diffusion, whereas the transport of glucose is facilitated by Glut transporters whose genes are often overexpressed in cancer cells (39, 40).

In this model, the expressions from Smallbone (35) were used for the uptake of O_2 and glucose in normal and cancer cells.

$$\text{Uptake}_{O_2} = [O_2]_{\text{extracellular}} \times K_{O_2}. \tag{B}$$

$$\text{Uptake}_{\text{Glucose}} = [\text{Glu}]_{\text{extracellular}} \times K_{\text{Glu}}. \tag{C}$$

K_{O_2} is the same for both normal and cancer cells, and K_{Glu} varies depending on the type of cancer cell. In this work, the values used for K_{Glu} in tumors were increased 10-, 50-, and 100-fold compared with normal cells, reflecting the increase in glucose metabolism.

The energetic metabolism was restricted to glycolysis and tricarboxylic acid cycle. All glucose taken up by the cell was considered to be primarily metabolized into ATP and CO_2. The excess of glucose not consumed in respiration is converted into ATP and lactic acid.

$$\text{Glucose} + 6 \times O_2 \Rightarrow 36 \times \text{ATP} + 6 \times CO_2. \tag{D}$$

$$\text{Glucose} \Rightarrow 2 \times \text{Lactate} + 2 \times H^+ + 2 \times \text{ATP}. \tag{E}$$

After 50 metabolic steps (500 diffusion steps), the fate of each cell was decided based on pHe and ATP production:

- If the pHe is lower than the threshold, the cell dies.
- If the ATP production is lower than the threshold for survival (0.85 μmol/L/s), the cell dies (35).
- Should the ATP production rate be above this value, the cell survives with a probability of duplication increasing with ATP production rate, reaching 100% for a value of 8.5 μmol/L/s or higher (35).
- Replication was allowed if there is empty space in the vicinity of the cell (any of the six faces of the cubic volume).

Blood vessels are represented as parallel horizontal lines with a cross section of one cell of area crossing the simulation space separated by five cells, which represents a distance of 125 μm between two blood vessels (34). There are no blood vessels in the tumor tissue because this model consists of micrometastasis.

The concentrations of the species in blood and their diffusion coefficients are listed in Supplementary Tables S1 to S5. The numerical method for calculating the effect of pH buffers is described in Supplementary data.

Results

Validation of Computer Model

The first step in this work was to validate the computer model. This was done by comparing the curves of pHe, O_2, CO_2, and glucose concentrations in interstitial fluid, both in tumor and in healthy tissue, with data from previously published experiments.

Supplementary Fig. S1 depicts profiles of extracellular glucose, extracellular O_2, extracellular CO_2, and pHe in the tumor and healthy tissue. All charts correspond to measurements along the top horizontal line, spanning from the center of tumor adjacent to the healthy tissue (Fig. 2, *horizontal line from A to B*).

pO_2. The results from our simulations are consistent with previous measurements (3) that showed a decrease in *p*O_2 from

serum levels to practically zero in a distance of 200 μm (corresponding to eight cells in this computer model). In our model, this profile remained unchanged, irrespective to the addition of buffers (data not shown) or the glycolytic phenotype of the cancer cells simulated (Supplementary Fig. S1).

Glucose. The simulations showed a slight decrease in the concentration of glucose in the healthy tissue (Supplementary Fig. S1) because the cells are further away from blood vessels. There was a steeper decrease in the availability of glucose further into the tumor tissue due to both the increased uptake of glucose and the lack of vascularization, as predicted by other models (35).

pCO_2. The CO_2 concentration curve (Supplementary Fig. S1) showed increased levels of carbon dioxide in cells located further from blood vessels. The levels of CO_2 in tumor were between 25% and 125% higher than in blood serum, which is in accordance with values previously measured *in vivo* (32, 33).

pHe. The pHe of the tumors in our model decreased as a function of the distance from the blood vessels and also with the increased metabolism of glucose into lactic acid (Supplementary Fig. S1). In the three tumor phenotypes considered, there was no presence of necrotic core.
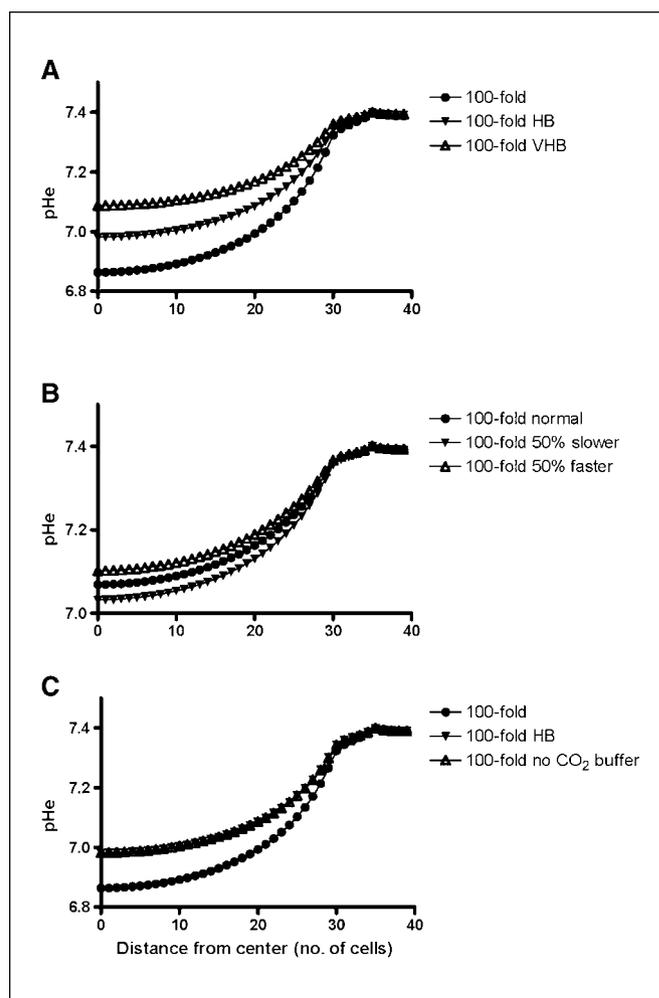
Figure 4. *A,* the effects of increased serum bicarbonate concentration on pHe gradient in tumors with 100-fold increase in glucose metabolism. *B,* the dependency of pHe gradient on the diffusion rate of a hypothetical buffer added to serum. *C,* the pHe gradient produced by a hypothetical non–CO_2-producing buffer compared with bicarbonate confirms that no noticeable difference exists if the other chemical properties (i.e., pK) are kept equal for the two buffers.

Figure 5. Dependency of pHe gradient on the value of the pK_a of the hypothetical buffer and comparison with no treatment. *Inset,* pHe increase (in pH units) in tumor center and tumor rim.
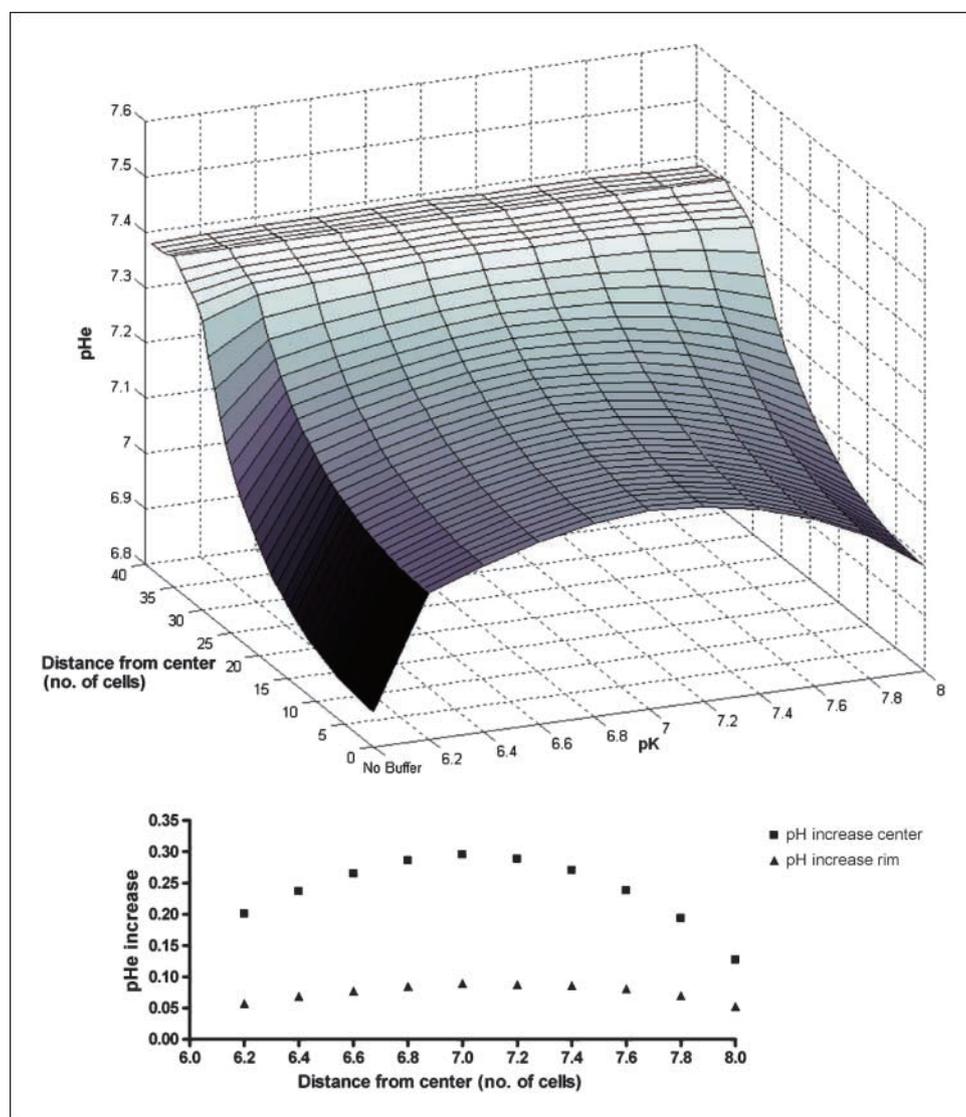
The pHe curves obtained in this work were consistent with the range of values found in previous *in vivo* experiments (3, 19, 41).

Simulation Results

The main purpose of this work was to evaluate the effect of addition of buffers to the blood serum in the pH of tumors. This was tested first using bicarbonate, which is readily available, and then comparing these results with hypothetical buffers of different pK_a values and diffusion coefficients.

Variation of bicarbonate concentration. The first test performed was an increase in the bicarbonate buffer concentration in blood serum, simulating the chronic ingestion of bicarbonate to evaluate the effect of increased doses of this buffer in the pHe in the tumor-host interface.

The curves of Fig. 4A represent the pHe gradient for the scenario of 100-fold increase in tumor glucose metabolism and three bicarbonate buffer concentrations, as shown in Supplementary Tables S1 to S3, representing a total of 25, 35, and 50 mmol/L of total buffer in blood serum, respectively (HCO_3^- + CO_2), identified as normal, high bicarbonate (HB), and very high bicarbonate (VHB)

concentrations. This is based on a range of serum concentrations that are achievable with ingestion of up to 70 g/d of $NaHCO_3$.

The results showed that for the less glycolytic tumor (10-fold increase), the highest bicarbonate concentration increased the pHe in the center of the tumor from 7.25 to 7.32, whereas the pHe in the rim increased from 7.38 to 7.39 (data not shown). In the most glycolytic tumors (100-fold increase), the same amount of bicarbonate resulted in an increase of pHe from 6.86 to 7.09 in the center and from 7.32 to 7.36 in the tumor rim.

In our computer model, the increases in total serum buffer concentration were 40% (HB) and 100% (VHB). The pHe profile for 40% increase (Fig. 4A) shows that the flattening of the pHe curve in tumors can be explained by the effect of bicarbonate.

Diffusion rate of hypothetical buffer. We next studied the effect of the diffusion rate of a hypothetical buffer used in conjunction with physiologic bicarbonate. A buffer that diffuses faster should more efficiently remove the excess of protons generated by the anaerobic glycolytic metabolism.

As before, simulations were done considering three different scenarios for the glucose metabolism of tumor cells. In all cases

(Fig. 4B), simulations were done under high serum levels of bicarbonate plus a hypothetical buffer with arbitrary pK_a 8 and three different diffusion rates: (a) diffusion rate of equal to that of the bicarbonate and CO_2, (b) 50% lower diffusion rate, and (c) 50% higher diffusion rate. Diffusion coefficients of these hypothetical buffers are shown in Supplementary Table S5.

As expected, the buffer with faster diffusion rate had the most noticeable effect on increasing the pHe. The differences between the slowest and the fastest buffers were 0.02, 0.05, and 0.08 pH unit in the tumor center for 10-fold, 50-fold (data not shown), and 100-fold glycolysis increases, respectively.

The effect of buffers with different diffusion rates is less noticeable than that observed for buffers with different pK_a; therefore, the diffusion rate does not seem to be the main parameter to be considered in the choice of an alternative buffer.

Bicarbonate combined with non–CO_2-generating buffer. Tumors are subject to heterogeneous external conditions; for instance, the rim might be exposed to normoxia whereas the core is hypoxic. We proposed that, although lactic acid is produced by anaerobic metabolism in the tumor center, a reasonable amount of CO_2 might be generated by respiration in the tumor rim. Due to lack of vascularization in the center of the tumor, carbon dioxide could accumulate inside the tumor, increasing acidity and reducing the efficiency of the bicarbonate buffer.

We compared the results of two scenarios: In the first case, a certain amount of bicarbonate was added to blood (10 mmol/L); in the second, the same amount was added in the form of a hypothetical buffer with pK_a of 6.1 and diffusion coefficients equal to the ones of bicarbonate buffer (A^- equal to HCO_3^- and AH equal to CO_2 diffusion, respectively). In both cases, the total buffer concentration in blood was the same (35 mmol/L). The concen-

trations for this buffer in blood serum are shown in Supplementary Table S4.

The simulations show that the pHe curve was not affected by the use of a non–CO_2-generating buffer (Fig. 4C). Considering that the diffusion rate of CO_2 is thrice faster than that of bicarbonate (Supplementary Table S1), we concluded that the limiting factor for the removal of free protons from the tumor is bicarbonate and not carbon dioxide.

Bicarbonate combined with buffers with different pK_a. We tested hypothetical buffers with the same concentration in blood serum (~ 18 mmol/L) with different pK_a values ranging from 6.2 to 8.0 at intervals of 0.2 pH unit (Fig. 5).

In all simulated tumors, the more noticeable effect was the buffer with pK_a of 7. This can be explained by the better efficiency of a pH buffer when used in a solution with pH in the range of 1 pH unit above or below the buffer pK_a.

The pH maintained in blood in this model is 7.4, and the pH in the center of the tumor is ~ 6.8; thus, a buffer with a pK_a close to the average of these values (~ 7) is supposedly more effective in absorbing the protons produced by the tumor.

Heterogeneity of tumor energetic metabolism. Tumors with increased glycolytic consumption on the order of magnitude of 50- or 100-fold presented an ATP production profile that reflected the decrease of the concentration of glucose on the environment. For these tumors, most of the energy was obtained from anaerobic glycolysis (>97% for 50-fold and >97.5% for 100-fold), even in the rim (data not shown).

Tumors with lower glucose uptake presented a combination of two behaviors: On the rim of the tumor (around three cells deep), the energy was obtained mostly by aerobic glucose metabolism (~ 92%), but at concentrations of oxygen below ~ 18 μmol/L, the
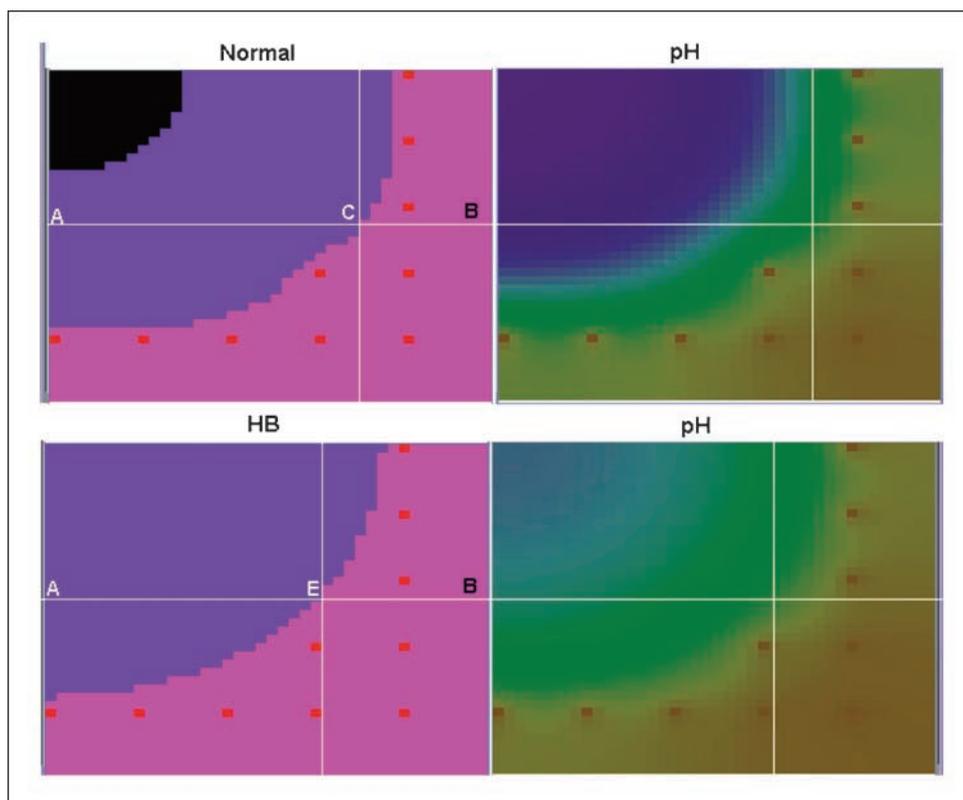
Figure 6. pHe distributions in and around tumors along with tumor growth after 20 generations with normal (*top row*) serum bicarbonate and with a 40% increase in concentration. As outlined in the text, pHe was much less acidic in the presence of increased serum buffer, resulting in a dramatic reduction in tumor invasion.

metabolism switched to anaerobic glycolysis, with >96% of ATP produced anaerobically at a distance of five cells away from tumor-healthy tissue interface (data not shown).

Tumor growth with increased concentrations of bicarbonate. To estimate the effect of increasing pH buffer availability and consequent reduction of the pHe gradient in tumor invasion, three scenarios were tested: normal bicarbonate concentration, HB concentration, and VHB concentration. The HB group corresponded to the bicarbonate concentration expected with ingestion of 40 g $NaHCO_3$ per day by a 70-kg man (see case report in Supplementary data). The HB group represented 40% of the VHB dose. Each scenario was run for 20 generations; at the end of each generation, the cells were allowed to duplicate, die, or remain unchanged.

The tumor growth and pHe gradients for normal and HB concentrations are depicted in Fig. 6 and Supplementary Fig. S2. With normal serum concentrations of bicarbonate, the tumor cells were highly acidic, created a significant peritumoral pHe gradient, and extensively invaded into the normal tissue. Addition of a moderate amount of bicarbonate in blood ($\sim 40\%$ increase in serum concentration) reduced the amount of intratumoral and peritumoral acidosis and almost completely eliminated tumor invasion (loss of only 12 healthy cells of >48,000). Treatment with higher bicarbonate (Supplementary Table S7) concentrations totally prevented invasion (no loss of normal cells). Note that both treatment scenarios also eliminated the necrotic tumor core that developed with normal bicarbonate concentrations—a potential imaging tumor biomarker for clinical trials.

Discussion

In this study, we used three-dimensional mathematical models to quantify the ability of systemic buffers to reduce the acidity of tumors and peritumoral normal tissue. The acid-mediated tumor invasion model suggests that reduction of the intratumoral and peritumoral pHe gradients will also reduce tumor growth and invasion. Our study finds that clinically achievable concentrations of $NaHCO_3$ can reduce malignant tumor growth and, thus, may have value as a clinical therapy.

The simulations show that increased concentration of serum bicarbonate can decrease intratumor and peritumor acidosis without altering blood pH. This might, at first, seem paradoxical, but we point out that this treatment is not "alkalization" but rather treatment with a physiologic buffer. The effect of the former is to produce a generalized increase in pH. By contrast, the effect of increasing the concentration of a physiologic buffer is to drive the entire system toward a normal pH (i.e., 7.35–7.45). Thus, regions that are at normal pH (such as blood) will not be affected although regions at abnormal pH (either acidic or alkaline) will tend toward physiologic values.

The results from our computer simulations are summarized below.

1. There is a linear relationship between the amount of bicarbonate in blood and the pHe in tumors of the size simulated in this work, although the pH in blood remains unchanged.
2. The use of a non–CO_2-generating buffer with the same pK_a and diffusion rates as bicarbonate does not provide advantages over bicarbonate, indicating that the by-product carbon dioxide is not the limiting factor in the efficiency of a bicarbonate buffer.

3. The pK_a of a hypothetical buffer is the most important characteristic on its effect on the tumor pHe. The proposed pK_a in this study is ~ 7.
4. The diffusion coefficient of a hypothetical buffer generates less noticeable effects when compared with different pK_a and, thus, is not the main parameter to be considered in the choice of an alternative buffer.
5. Moderate increases in the serum $NaHCO_3$ concentrations will substantially reduce intratumoral and peritumoral acidity, which will virtually eliminate tumor invasion into normal adjacent tissue, resulting in stable tumor size.

The results obtained in this work are consistent with the data measured in window chambers in the companion article (42) and previous work (32). The size of the tumor in the simulations is comparable with those measured in the experimental window chamber model (diameters of 1.5 mm for the simulated tumor and 1.4 mm for the window chamber), and the pHe gradients from Fig. 4 fit quantitatively the experimental curves [6.86 at the center and 7.09 at the rim for the simulated tumors (Fig. 4) and 6.9 at the center and 7.15 at the rim measured experimentally (19, 42)]. The pHe curves in and around tumors obtained in the simulations with normal and elevated serum concentrations of $NaHCO_3$ can be compared with experimentally determined acid concentrations (42). In this study, green fluorescent protein–labeled MDA-mb-231 tumors were grown in window chambers in severe combined immunodeficient mice. Bicarbonate concentrations were increased by adding 200 mmol/L $NaHCO_3$ to the drinking water. This was calculated to be the equivalent of a daily dose of 37 g in a 70-kg human. The pHe gradient in the tumor and peritumoral normal tissues was measured using fluorescent ratio imaging. As shown in Fig. 5 of our companion article (42), the pHe gradients of the tumor increased from 0.1 to 0.2 pH unit when the bicarbonate was added to the water, remarkably similar to the changes observed in the computer simulations.

The clinical feasibility of chronic ingestion of bicarbonate to reduce tumor invasion is an open question. Interestingly, $NaHCO_3$ is readily available in grocery stores (as baking soda) and in over-the-counter preparations for clinical use as an antacid. The recommended daily dose is five teaspoons a day, which is 25 to 50 g (depending on how heaped the teaspoon is). This dose has been administered chronically (i.e., >1 year) in patients with renal tubular acidosis and sickle cell anemia without adverse affects (43, 44). Finally, in Supplementary data, we include the experience of a 79-year-old man with widely metastatic renal cancer at the Moffitt Cancer Center. After failing first-line treatment, he discontinued conventional therapy and began a self-administered course of vitamins, supplements, and 60 g of bicarbonate mixed in water daily. As of this submission, he has remained well with stable tumor for 10 months. Although little information can be gained from a single case report, we do note that he has tolerated the VHB administration used in our simulations without complication for nearly 1 year, suggesting that it is clinically feasible.

An interesting result of the simulations is that the use of buffers with pK_a of ~ 7 might yield to results similar or better than those obtained with bicarbonate (pK_a, 6.1; ref. 45). Candidate buffers could be cholamine chloride (pK_a, 7.1), BES (pK_a, 7.15), TES (pK_a, 7.5), or HEPES (pK_a, 7.55; ref. 46). However, the effect of these buffers *in vivo* must be evaluated because bicarbonate is a natural buffer controlled by the organism through ventilation and excretion in kidneys; the use of an artificial buffer might lead to side effects and toxicity.

In conclusion, our study, using mathematical models informed by realistic parameter values (47–50), finds that p.o. administration of clinically feasible amounts of NaHCO$_3$ may be sufficient to increase the acidic intratumoral and peritumoral pHe in small tumors. Furthermore, the consequent changes in the tumor-host dynamics may inhibit tumor growth and invasion. Our results suggest further experimental exploration of systemic administration of pH buffers as a novel cancer therapy is warranted.

Disclosure of Potential Conflicts of Interest

Acknowledgments

References

1. Gillies RJ, Raghunand N, Garcia-Martin ML, Gatenby RA. pH imaging. A review of pH measurement methods and applications in cancers. IEEE Eng Med Biol Mag 2004;23:57–64.

2. Gillies RJ, Raghunand N, Karczmar GS, Bhujwalla ZM. MRI of the tumor microenvironment. J Magn Reson Imaging 2002;16:430–50.

3. Helmlinger G, Yuan F, Dellian M, Jain RK. Interstitial pH and pO_2 gradients in solid tumors in vivo: high-resolution measurements reveal a lack of correlation. Nat Med 1997;3:177–82.

4. Gallagher FA, Kettunen MI, Day SE, et al. Magnetic resonance imaging of pH in vivo using hyperpolarized ^{13}C-labelled bicarbonate. Nature 2008;453:940–3.

5. Gatenby RA, Gillies RJ. Why do cancers have high aerobic glycolysis? Nat Rev Cancer 2004;4:891–9.

6. Moellering RE, Black KC, Krishnamurty C, et al. Acid treatment of melanoma cells selects for invasive phenotypes. Clin Exp Metastasis 2008;25:411–25.

7. Rofstad EK, Mathiesen B, Kindem K, Galappathi K. Acidic extracellular pH promotes experimental metastasis of human melanoma cells in athymic nude mice. Cancer Res 2006;66:6699–707.

8. Cuvier C, Jang A, Hill RP. Exposure to hypoxia, glucose starvation and acidosis: effect on invasive capacity of murine tumor cells and correlation with cathepsin (L + B) secretion. Clin Exp Metastasis 1997;15:19–25.

9. Kalliomaki T, Hill RP. Effects of tumour acidification with glucose+MIBG on the spontaneous metastatic potential of two murine cell lines. Br J Cancer 2004;90:1842–9.

10. Rozhin J, Sameni M, Ziegler G, Sloane BF. Pericellular pH affects distribution and secretion of cathepsin B in malignant cells. Cancer Res 1994;54:6517–25.

11. Xu L, Fidler IJ. Acidic pH-induced elevation in interleukin 8 expression by human ovarian carcinoma cells. Cancer Res 2000;60:4610–6.

12. Shi Q, Le X, Wang B, et al. Regulation of vascular endothelial growth factor expression by acidosis in human cancer cells. Oncogene 2001;20:3751–6.

13. Swietach P, Vaughan-Jones RD, Harris AL. Regulation of tumor pH and the role of carbonic anhydrase 9. Cancer Metastasis Rev 2007;26:299–310.

14. Ceccarini C, Eagle H. pH as a determinant of cellular growth and contact inhibition. Proc Natl Acad Sci U S A 1971;68:229–33.

15. Park HJ, Lyons JC, Ohtsubo T, Song CW. Acidic environment causes apoptosis by increasing caspase activity. Br J Cancer 1999;80:1892–7.

16. Williams AC, Collard TJ, Paraskeva C. An acidic environment leads to p53 dependent induction of apoptosis in human adenoma and carcinoma cell lines: implications for clonal selection during colorectal carcinogenesis. Oncogene 1999;18:3199–204.

17. Lardner A. The effects of extracellular pH on immune function. J Leukoc Biol 2001;69:522–30.

18. Gatenby RA, Gawlinski ET. A reaction-diffusion model of cancer invasion. Cancer Res 1996;56:5745–53.

19. Gatenby RA, Gawlinski ET, Gmitro AF, Kaylor B, Gillies RJ. Acid-mediated tumor invasion: a multidisciplinary study. Cancer Res 2006;66:5216–23.

20. Yasuda S, Fujii H, Nakahara T, et al. 18F-FDG PET detection of colonic adenomas. J Nucl Med 2001;42:989–92.

21. Abbey CK, Borowsky AD, McGoldrick ET, et al. In vivo positron-emission tomography imaging of progression and transformation in a mouse model of mammary neoplasia. Proc Natl Acad Sci U S A 2004;101:11438–43.

22. Schwarzbach MH, Hinz U, Dimitrakopoulou-Strauss A, et al. Prognostic significance of preoperative [^{18}F]fluorodeoxyglucose (FDG) positron emission tomography (PET) imaging in patients with resectable soft tissue sarcomas. Ann Surg 2005;241:286–94.

23. Schwartz DL, Rajendran J, Yueh B, et al. FDG-PET prediction of head and neck squamous cell cancer outcomes. Arch Otolaryngol Head Neck Surg 2004;130:1361–7.

24. Vansteenkiste J, Fischer BM, Dooms C, Mortensen J. Positron-emission tomography in prognostic and therapeutic assessment of lung cancer: systematic review. Lancet Oncol 2004;5:531–40.

25. Walenta S, Wetterling M, Lehrke M, et al. High lactate levels predict likelihood of metastases, tumor recurrence, and restricted patient survival in human cervical cancers. Cancer Res 2000;60:916–21.

26. Schwickert G, Walenta S, Sundfor K, Rofstad EK, Mueller-Klieser W. Correlation of high lactate levels in human cervical cancer with incidence of metastasis. Cancer Res 1995;55:4757–9.

27. Kolev Y, Uetake H, Takagi Y, Sugihara K. Lactate dehydrogenase-5 (LDH-5) expression in human gastric cancer: association with hypoxia-inducible factor (HIF-1α) pathway, angiogenic factors production and poor prognosis. Ann Surg Oncol 2008;15:2336–44.

28. Hui EP, Chan AT, Pezzella F, et al. Coexpression of hypoxia-inducible factors 1α and 2α, carbonic anhydrase IX, and vascular endothelial growth factor in nasopharyngeal carcinoma and relationship to survival. Clin Cancer Res 2002;8:2595–604.

29. Choi SW, Kim JY, Park JY, Cha IH, Kim J, Lee S. Expression of carbonic anhydrase IX is associated with postoperative recurrence and poor prognosis in surgically treated oral squamous cell carcinoma. Hum Pathol 2008;39:1317–22.

30. Nomura T, Katunuma N. Involvement of cathepsins in the invasion, metastasis and proliferation of cancer cells. J Med Invest 2005;52:1–9.

31. Benoy IH, Salgado R, Van Dam P, et al. Increased serum interleukin-8 in patients with early and metastatic breast cancer correlates with early dissemination and survival. Clin Cancer Res 2004;10:7157–62.

32. Gullino PM, Grantham FH, Smith SH, Haggerty AC. Modifications of the acid-base status of the internal milieu of tumors. J Natl Cancer Inst 1965;34:857–69.

33. Helmlinger G, Sckell A, Dellian M, Forbes NS, Jain RK. Acid production in glycolysis-impaired tumors provides new insights into tumor metabolism. Clin Cancer Res 2002;8:1284–91.

34. Patel AA, Gawlinski ET, Lemieux SK, Gatenby RA. A cellular automaton model of early tumor growth and invasion. J Theor Biol 2001;213:315–31.

35. Smallbone K, Gatenby RA, Gillies RJ, Maini PK, Gavaghan DJ. Metabolic changes during carcinogenesis: potential impact on invasiveness. J Theor Biol 2007;244:703–13.

36. Ferreira SC, Jr., Martins ML, Vilela MJ. Reaction-diffusion model for the growth of avascular tumor. Phys Rev E Stat Nonlin Soft Matter Phys 2002;65:021907.

37. Kanamaru H, Muranaka K, Mori H, Akino H, Arai Y, Okada K. Analysis of histological heterogeneity in renal cell carcinoma: tumor size-related histological change and its prognostic significance. Int J Urol 1996;3:256–60.

38. Warburg O. On respiratory impairment in cancer cells. Science 1956;124:269–70.

39. Kunkel M, Reichert TE, Benz P, et al. Overexpression of Glut-1 and increased glucose metabolism in tumors are associated with a poor prognosis in patients with oral squamous cell carcinoma. Cancer 2003;97:1015–24.

40. Wykoff CC, Beasley N, Watson PH, et al. Expression of the hypoxia-inducible and tumor-associated carbonic anhydrases in ductal carcinoma in situ of the breast. Am J Pathol 2001;158:1011–9.

41. Martin GR, Jain RK. Noninvasive measurement of interstitial pH profiles in normal and neoplastic tissue using fluorescence ratio imaging microscopy. Cancer Res 1994;54:5670–4.

42. Robey IF, Baggett BK, Kirkpatrick ND, et al. Bicarbonate increases tumor pH and inhibits spontaneous metastases. Cancer Res 2009;69:2260–8.

43. Booth BE, Gates J, Morris RC, Jr. Grocery store baking soda. A source of sodium bicarbonate in the management of chronic metabolic acidosis. Clin Pediatr (Phila) 1984;23:94–6.

44. Mann JR, Stuart J. Sodium bicarbonate prophylaxis of sickle cell crisis. Pediatrics 1974;53:414–6.

45. Putnam RW, Roos A. Which value for the first dissociation constant of carbonic acid should be used in biological work? Am J Physiol 1991;260:C1113–6.

46. Good NE, Winget GD, Winter W, Connolly TN, Izawa S, Singh RM. Hydrogen ion buffers for biological research. Biochemistry 1966;5:467–77.

47. Tanaka S, Meiselman HH, Engel E, et al. Regional differences in H$^+$, HCO$_3^-$, and CO$_2$ diffusion through native porcine gastroduodenal mucus. Dig Dis Sci 2002;47:967–73.

48. Groebe K, Erz S, Mueller-Klieser W. Glucose diffusion coefficients determined from concentration profiles in EMT6 tumor spheroids incubated in radioactively labeled L-glucose. Adv Exp Med Biol 1994;361:619–25.

49. Nichols MG, Foster TH. Oxygen diffusion and reaction kinetics in the photodynamic therapy of multicell tumour spheroids. Phys Med Biol 1994;39:2161–81.

50. Mizumori M, Meyerowitz J, Takeuchi T, et al. Epithelial carbonic anhydrases facilitate pCO2 and pH regulation in rat duodenal mucosa. J Physiol 2006;573:827–42.